BPS Dendroscopy on Local Calabi-Yau Threefolds

Boris Pioline

LPTHE
LABORATOIRE DE PHYSIQUE THEORIQUE ET HAUTES ENERGIES

cnrs

SORBONNE UNIVERSITÉ

String-Math 2022, 14/07/2022

Work in progress with Pierrick Bousseau, Pierre Descombes and Bruno Le Floch

$\delta\varepsilon\nu\delta\rho o\nu$= tree

Dentrology

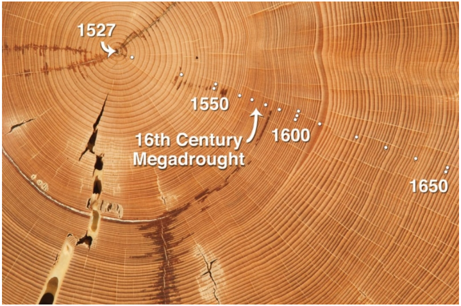

Dendrochronology

δενδροσκοπια= analyzing the BPS spectrum in terms of attractor flow trees

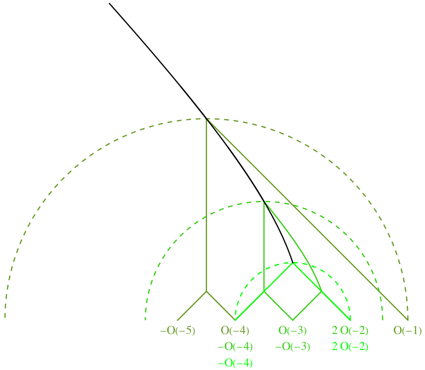

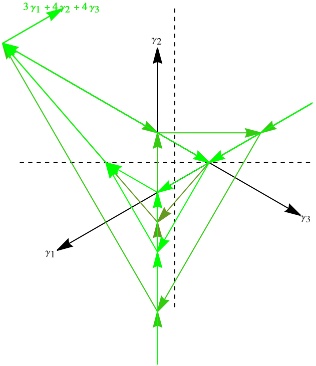

Attractor flow trees on $K_{\mathbb{P}^2}$, $\gamma = [1, 0, -3)$, $\mathcal{M} = \mathrm{Hilb}_4\mathbb{P}^2$

- In type IIA string theory compactified on a Calabi-Yau threefold X, the BPS spectrum consists of bound states of D6-D4-D2-D0 branes, described mathematically by objects E in the derived category of coherent sheaves $\mathcal{C} = D^b\mathrm{Coh}(X)$ *[Douglas'01]*

Introduction

- In type IIA string theory compactified on a Calabi-Yau threefold X, the BPS spectrum consists of bound states of D6-D4-D2-D0 branes, described mathematically by objects E in the derived category of coherent sheaves $\mathcal{C} = D^b\mathrm{Coh}(X)$ *[Douglas'01]*
- The BPS index or Donaldson-Thomas invariant $\Omega_z(\gamma)$ counts stable states with charge $\gamma = \mathrm{ch}\, E \in H_{\mathrm{even}}(X, \mathbb{Q})$ saturating the BPS bound $M(\gamma) \geq |Z(\gamma)|$, where $Z \in \mathrm{Hom}(\Gamma, \mathbb{C})$ depends on the complexified Kähler moduli $z \in \mathcal{M}$.

Introduction

- In type IIA string theory compactified on a Calabi-Yau threefold X, the BPS spectrum consists of bound states of D6-D4-D2-D0 branes, described mathematically by objects E in the derived category of coherent sheaves $\mathcal{C} = D^b\mathrm{Coh}(X)$ *[Douglas'01]*
- The BPS index or Donaldson-Thomas invariant $\Omega_z(\gamma)$ counts stable states with charge $\gamma = \mathrm{ch}\, E \in H_{\mathrm{even}}(X, \mathbb{Q})$ saturating the BPS bound $M(\gamma) \geq |Z(\gamma)|$, where $Z \in \mathrm{Hom}(\Gamma, \mathbb{C})$ depends on the complexified Kähler moduli $z \in \mathcal{M}$.
- $\Omega_z(\gamma)$ is locally constant on $\mathcal{M}$, but can jump across real codimension one walls of marginal stability $\mathcal{W}(\gamma_1, \gamma_2) \subset \mathcal{M}$, where the phases of the central charges $Z(\gamma_1)$ and $Z(\gamma_2)$ with $\gamma = m_1\gamma_1 + m_2\gamma_2$ become aligned *[Kontsevich Soibelman'08, Joyce Song'08]*

Introduction

- In type IIA string theory compactified on a Calabi-Yau threefold X, the BPS spectrum consists of bound states of D6-D4-D2-D0 branes, described mathematically by objects E in the derived category of coherent sheaves $\mathcal{C} = D^b\mathrm{Coh}(X)$ *[Douglas'01]*
- The BPS index or Donaldson-Thomas invariant $\Omega_z(\gamma)$ counts stable states with charge $\gamma = \mathrm{ch}\, E \in H_{\mathrm{even}}(X, \mathbb{Q})$ saturating the BPS bound $M(\gamma) \geq |Z(\gamma)|$, where $Z \in \mathrm{Hom}(\Gamma, \mathbb{C})$ depends on the complexified Kähler moduli $z \in \mathcal{M}$.
- $\Omega_z(\gamma)$ is locally constant on $\mathcal{M}$, but can jump across real codimension one walls of marginal stability $\mathcal{W}(\gamma_1, \gamma_2) \subset \mathcal{M}$, where the phases of the central charges $Z(\gamma_1)$ and $Z(\gamma_2)$ with $\gamma = m_1\gamma_1 + m_2\gamma_2$ become aligned *[Kontsevich Soibelman'08, Joyce Song'08]*
- Physically, multi-centered black hole solutions (dis)appear across the wall *[Denef Moore '07, ..., Manschot BP Sen '11]*.

BPS spectrum on local surfaces

- For a non-compact CY3 of the form $X = K_S$ where S is a complex Fano surface, there is an injection $\iota_* : D^b \operatorname{Coh}(S) \to D^b_c(X)$ lifting an object E with Chern character $\gamma = [r, d, \mathrm{ch}_2]$ to a bound state of r D4-branes wrapped on S, c D2-branes and ch_2 D0-branes.

BPS spectrum on local surfaces

- For a non-compact CY3 of the form $X = K_S$ where S is a complex Fano surface, there is an injection $\iota_* : D^b \operatorname{Coh}(S) \to D^b_c(X)$ lifting an object E with Chern character $\gamma = [r, d, \mathrm{ch}_2]$ to a bound state of r D4-branes wrapped on S, c D2-branes and ch_2 D0-branes.
- At large volume, the central charge is quadratic in complexified Kähler moduli $z^a = b^a + \mathrm{i} t^a$,

$$Z(\gamma) \sim -\int_S e^{-z^a H_a} \operatorname{ch} E = -r\, z^a Q_{ab} z^b + z^a d_a - \mathrm{ch}_2$$

  $\Omega_z(\gamma)$ reduces to the Gieseker index $\Omega_\infty(\gamma)$, given (up to sign) by the Euler number of the moduli space of Gieseker semi-stable sheaves on S with Chern character γ.

BPS spectrum on local surfaces

- For a non-compact CY3 of the form $X = K_S$ where S is a complex Fano surface, there is an injection $\iota_* : D^b\,\mathrm{Coh}(S) \to D^b_c(X)$ lifting an object E with Chern character $\gamma = [r, d, \mathrm{ch}_2]$ to a bound state of r D4-branes wrapped on S, c D2-branes and ch_2 D0-branes.
- At large volume, the central charge is quadratic in complexified Kähler moduli $z^a = b^a + \mathrm{i}t^a$,

$$Z(\gamma) \sim -\int_S e^{-z^a H_a}\,\mathrm{ch}\,E = -r\,z^a Q_{ab} z^b + z^a d_a - \mathrm{ch}_2$$

  $\Omega_z(\gamma)$ reduces to the Gieseker index $\Omega_\infty(\gamma)$, given (up to sign) by the Euler number of the moduli space of Gieseker semi-stable sheaves on S with Chern character γ.
- At finite volume, Z receives worldsheet instanton corrections computable by mirror symmetry. Can we determine $\Omega_z(\gamma)$ anywhere, and understand what are BPS states really "made of" ?

Outline

1. Introduction
2. Kähler moduli space of $K_{\mathbb{P}^2}$
3. Attractor flow trees and scattering diagrams
4. Large volume scattering diagram
5. Towards the exact scattering diagram

Outline

Kähler moduli space of $K_{\mathbb{P}^2}$

- The Kähler moduli space of $K_{\mathbb{P}^2}$ is the modular curve $X_1(3) = \mathbb{H}/\Gamma_1(3)$ parametrizing elliptic curves with level structure. It admits two cusps LV, C and one elliptic point o of order 3.

Kähler moduli space of $K_{\mathbb{P}^2}$

- The Kähler moduli space of $K_{\mathbb{P}^2}$ is the modular curve $X_1(3) = \mathbb{H}/\Gamma_1(3)$ parametrizing elliptic curves with level structure. It admits two cusps LV, C and one elliptic point o of order 3.
- The universal cover is parametrized by $\tau \in \mathbb{H}$:

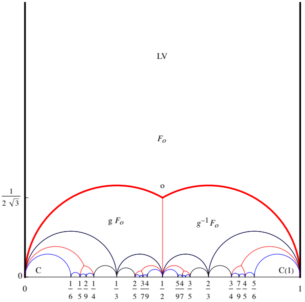

$$
\begin{aligned}
Z_\tau(\gamma) &= -rT_D(\tau) + dT(\tau) - \mathrm{ch}_2 \\
T &= \int_\ell \lambda \\
T_D &= \int_{\ell_D} \lambda
\end{aligned}
$$

λ holomorphic one-form with logarithmic singularities on $\mathcal{E}_\tau$

Central charge as Eichler integral

- Since $\partial_\tau \lambda$ is holomorphic, its periods are proportional to $(1, \tau)$. Integrating on a path from o to τ, one finds the Eichler-type integral

$$\boxed{\begin{pmatrix} T \\ T_D \end{pmatrix} = \begin{pmatrix} 1/2 \\ 1/3 \end{pmatrix} + \int_{\tau_o}^{\tau} \begin{pmatrix} 1 \\ u \end{pmatrix} C(u)\, \mathrm{d}u}$$

where $C(\tau) = \frac{\eta(\tau)^9}{\eta(3\tau)^3}$ is a weight 3 modular form for $\Gamma_1(3)$.

Central charge as Eichler integral

- Since $\partial_\tau \lambda$ is holomorphic, its periods are proportional to $(1, \tau)$. Integrating on a path from o to τ, one finds the Eichler-type integral

$$\boxed{\begin{pmatrix} T \\ T_D \end{pmatrix} = \begin{pmatrix} 1/2 \\ 1/3 \end{pmatrix} + \int_{\tau_o}^{\tau} \begin{pmatrix} 1 \\ u \end{pmatrix} C(u)\,\mathrm{d}u}$$

  where $C(\tau) = \frac{\eta(\tau)^9}{\eta(3\tau)^3}$ is a weight 3 modular form for $\Gamma_1(3)$.

- This provides an computationally efficient analytic continuation of Z_τ throughout $\mathbb{H}$, and gives access to monodromies:

$$\tau \mapsto \frac{a\tau + b}{c\tau + d} \qquad \begin{pmatrix} 1 \\ T \\ T_D \end{pmatrix} \mapsto \begin{pmatrix} 1 & 0 & 0 \\ m & d & c \\ m_D & b & a \end{pmatrix} \cdot \begin{pmatrix} 1 \\ T \\ T_D \end{pmatrix}$$

  where (m, m_D) are period integrals of C from τ_o to $\frac{a\tau_o - b}{c\tau_o - d}$.

Central charge as Eichler integral

- At large volume, using $C = 1 - 9q + \dots$ one finds

$$T = \tau + \mathcal{O}(q), \quad T_D = \frac{1}{2}\tau^2 + \frac{1}{8} + \mathcal{O}(q)$$

Central charge as Eichler integral

- At large volume, using $C = 1 - 9q + \ldots$ one finds

$$T = \tau + \mathcal{O}(q), \quad T_D = \frac{1}{2}\tau^2 + \frac{1}{8} + \mathcal{O}(q)$$

- For τ_2 large enough, one can use the $GL(2,\mathbb{R})^+$ action on space of Bridgeland stability conditions to absorb the $\mathcal{O}(q)$ corrections:

$$Z^{LV}_{(s,t)}(\gamma) = -\frac{r}{2}(s + \mathrm{i}t)^2 + d(s + \mathrm{i}t) - \mathrm{ch}_2 \ ,$$

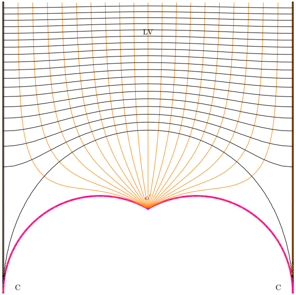

$$s = \frac{\operatorname{Im} T_D}{\operatorname{Im} T} \ , \quad \mu = \frac{d}{r}$$

$$\frac{1}{2}(s^2 + t^2) = -\frac{\operatorname{Im}(T \bar{T}_D)}{\operatorname{Im} T}$$

$$\mathcal{A} = \{E \xrightarrow{d} F, \mu(E) < s, \mu(F) \geq s\}$$

[Bayer Macri'11]

Quiver for $K_{\mathbb{P}^2}$

- Near the orbifold point $\tau_o = -\frac{1}{2} + \frac{\mathrm{i}}{2\sqrt{3}}$, the BPS spectrum is governed by a quiver with potential:

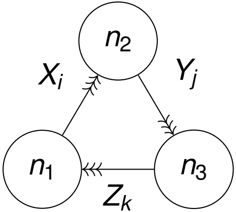

$$W = \sum \epsilon_{ijk} X_i Y_j Z_k$$

$$\begin{array}{lllll} E_1 & = & \mathcal{O} & & \gamma_1 = [1,0,0] \\ E_2 & = & \Omega(1)[1], & & \gamma_2 = [-2,1,\frac{1}{2}] \\ E_3 & = & \mathcal{O}(-1)[2] & & \gamma_3 = [1,-1,\frac{1}{2}] \\ & & r = & & 2n_2 - n_1 - n_3 \\ & & d = & & n_3 - n_2 \\ & & \mathrm{ch}_2 = & & -\frac{1}{2}(n_2 + n_3) \end{array}$$

- The BPS index $\Omega_\tau(\gamma)$ coincides with the (signed) Euler number $\Omega_\zeta(\gamma)$ of the moduli space of King semi-stable representations of dimension $\gamma = (n_1, n_2, n_3)$, with FI-parameters $\theta_i = \mathrm{Im} Z_\tau(\gamma_i)$.

Attractor conjecture for $K_{\mathbb{P}^2}$

- In the chamber $\theta_1 > 0, \theta_3 < 0$, the arrows Z_k vanish in any stable representation, and (Q, W) reduces to the Beilinson quiver describing normalized torsion-free sheaves on $\mathbb{P}^2$:

$$n_1 \xrightarrow{X_i} n_2 \xrightarrow{Y_j} n_3 \qquad \epsilon_{ijk} X^i Y^j = 0$$

Douglas Fiol Romelsberger'00

Attractor conjecture for $K_{\mathbb{P}^2}$

- In the chamber $\theta_1 > 0, \theta_3 < 0$, the arrows Z_k vanish in any stable representation, and (Q, W) reduces to the Beilinson quiver describing normalized torsion-free sheaves on $\mathbb{P}^2$:

$$n_1 \xrightarrow{X_i} n_2 \xrightarrow{Y_j} n_3 \qquad \epsilon_{ijk} X^i Y^j = 0$$

Douglas Fiol Romelsberger'00

- In *[Beaujard BP Manschot'20]*, we showed that the attractor index $\Omega_\star(\gamma) := \Omega_{\langle\gamma,-\rangle}(\gamma)$ vanishes except for $\gamma = \gamma_i$ or $\gamma \propto \gamma_1 + \gamma_2 + \gamma_3$.

Attractor conjecture for $K_{\mathbb{P}^2}$

- In the chamber $\theta_1 > 0, \theta_3 < 0$, the arrows Z_k vanish in any stable representation, and (Q, W) reduces to the Beilinson quiver describing normalized torsion-free sheaves on $\mathbb{P}^2$:

$$n_1 \xrightarrow{X_i} n_2 \xrightarrow{Y_j} n_3 \qquad \epsilon_{ijk} X^i Y^j = 0$$

Douglas Fiol Romelsberger'00

- In *[Beaujard BP Manschot'20]*, we showed that the attractor index $\Omega_\star(\gamma) := \Omega_{\langle\gamma,-\rangle}(\gamma)$ vanishes except for $\gamma = \gamma_i$ or $\gamma \propto \gamma_1 + \gamma_2 + \gamma_3$.
- Moreover, the anti-attractor index $\Omega_x(\gamma) := \Omega_{-\langle\gamma,-\rangle}(\gamma)$ coincide with the Gieseker index $\Omega_\infty(\gamma)$, provided $-r < d \leq 0$.

Attractor conjecture for $K_{\mathbb{P}^2}$

- In the chamber $\theta_1 > 0, \theta_3 < 0$, the arrows Z_k vanish in any stable representation, and (Q, W) reduces to the Beilinson quiver describing normalized torsion-free sheaves on $\mathbb{P}^2$:

$$\begin{tikzcd} n_1 \arrow[r, "X_i", shift left=2] \arrow[r] \arrow[r, shift right=2] & n_2 \arrow[r, "Y_j", shift left=2] \arrow[r] \arrow[r, shift right=2] & n_3 \end{tikzcd} \qquad \epsilon_{ijk} X^i Y^j = 0$$

Douglas Fiol Romelsberger'00

- In *[Beaujard BP Manschot'20]*, we showed that the attractor index $\Omega_\star(\gamma) := \Omega_{\langle\gamma,-\rangle}(\gamma)$ vanishes except for $\gamma = \gamma_i$ or $\gamma \propto \gamma_1 + \gamma_2 + \gamma_3$.
- Moreover, the anti-attractor index $\Omega_x(\gamma) := \Omega_{-\langle\gamma,-\rangle}(\gamma)$ coincide with the Gieseker index $\Omega_\infty(\gamma)$, provided $-r < d \leq 0$.
- A similar conjecture for $\Omega_\star(\gamma)$ holds for any toric CY3, giving in principle access to DT invariants $\Omega_\zeta(\gamma)$ for any $\zeta \in \mathbb{R}^{Q_0}$ *[Mozgovoy BP'20; Descombes'21]*

Outline

1. Introduction
2. Kähler moduli space of $K_{\mathbb{P}^2}$
3. Attractor flow trees and scattering diagrams
4. Large volume scattering diagram
5. Towards the exact scattering diagram

The Attractor Flow Tree formula for quivers

- The Attractor Flow Tree Formula expresses the BPS index $\Omega_\theta(\gamma)$ for any (generic) $\theta \in \mathbb{R}^{Q_0}$ in terms of attractor indices by summing over all possible flow trees: schematically,

$$\Omega_\theta(\gamma) \sim \sum_{\gamma=\gamma_1+\dots+\gamma_n} \left(\sum_{T\in\mathcal{T}_\theta(\{\gamma_i\})} \prod_{v\in V_T} \langle \gamma_{L(v)}, \gamma_{R(v)} \rangle \right) \prod_{i=1}^{n} \Omega_\star(\gamma_i)$$

Denef '00; Denef Greene Raugas '01; Denef Moore'07; Manschot '10, Alexandrov BP'18

The Attractor Flow Tree formula for quivers

- The Attractor Flow Tree Formula expresses the BPS index $\Omega_\theta(\gamma)$ for any (generic) $\theta \in \mathbb{R}^{Q_0}$ in terms of attractor indices by summing over all possible flow trees: schematically,

$$\Omega_\theta(\gamma) \sim \sum_{\gamma=\gamma_1+\dots+\gamma_n} \left(\sum_{T\in\mathcal{T}_\theta(\{\gamma_i\})} \prod_{v\in V_T} \langle\gamma_{L(v)}, \gamma_{R(v)}\rangle \right) \prod_{i=1}^{n} \Omega_\star(\gamma_i)$$

Denef '00; Denef Greene Raugas '01; Denef Moore'07; Manschot '10, Alexandrov BP'18

- Here, a flow tree T is a binary rooted tree, with edges decorated with charges γ_e, such that $\gamma_v = \gamma_{L(v)} + \gamma_{R(v)}$ at each vertex, with charges γ_i assigned to the leaves and γ to the root.

The Attractor Flow Tree formula for quivers

- The Attractor Flow Tree Formula expresses the BPS index $\Omega_\theta(\gamma)$ for any (generic) $\theta \in \mathbb{R}^{Q_0}$ in terms of attractor indices by summing over all possible flow trees: schematically,

$$\Omega_\theta(\gamma) \sim \sum_{\gamma=\gamma_1+\cdots+\gamma_n} \left(\sum_{T\in\mathcal{T}_\theta(\{\gamma_i\})} \prod_{v\in V_T} \langle \gamma_{L(v)}, \gamma_{R(v)} \rangle \right) \prod_{i=1}^{n} \Omega_\star(\gamma_i)$$

Denef '00; Denef Greene Raugas '01; Denef Moore'07; Manschot '10, Alexandrov BP'18

- Here, a flow tree T is a binary rooted tree, with edges decorated with charges γ_e, such that $\gamma_v = \gamma_{L(v)} + \gamma_{R(v)}$ at each vertex, with charges γ_i assigned to the leaves and γ to the root.
- Each edge is embedded in $\mathbb{R}^{Q_0}$ along $\theta_v = \theta_{p(v)} + \lambda\langle\gamma_e, -\rangle$, $\lambda \geq 0$, such that the root vertex maps to θ, and $(\theta_v, \gamma_{L(v)}) = (\theta_v, \gamma_{R(v)}) = 0$ at each vertex.

Split attractor flows

- The physical picture is that typical multi-centered solutions in $\mathcal{N} = 2$ supergravity have a nested structure

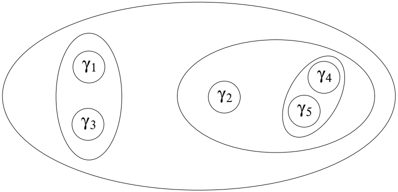

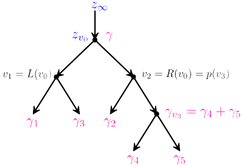

Split attractor flows

- The physical picture is that typical multi-centered solutions in $\mathcal{N}=2$ supergravity have a nested structure

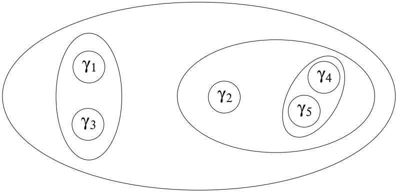

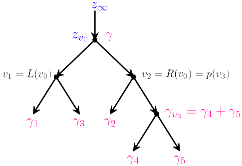

- The linear flow in θ originates from gradient flow for spherically symmetric black holes *[Ferrara Kallosh Strominger'95]*

$$r^2 \frac{\mathrm{d}z^i}{\mathrm{d}r} = -g^{i\bar{j}} \partial_{\bar{j}} |Z(\gamma)|^2$$

Split attractor flows

- The physical picture is that typical multi-centered solutions in $\mathcal{N}=2$ supergravity have a nested structure

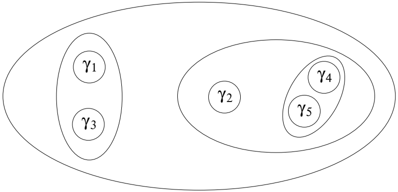

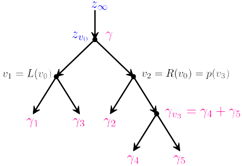

- The linear flow in θ originates from gradient flow for spherically symmetric black holes *[Ferrara Kallosh Strominger'95]*

$$r^2 \frac{\mathrm{d}z^i}{\mathrm{d}r} = -g^{i\bar{j}} \partial_{\bar{j}} |Z(\gamma)|^2$$

- At each level v, the average distance between the clusters of charge $\gamma_L(v)$ and $\gamma_R(v)$ is fixed, but the orientation in S^2 gives $|\langle \gamma_{L(v)}, \gamma_{R(v)} \rangle|$ degrees of freedom. In addition, each center of charge γ_i carries internal degrees of freedom counted by $\Omega_\star(\gamma_i)$.

Remarks

- In order to enforce Bose-Fermi statistics whenever two charges coincide, one should replace $\Omega_\theta(\gamma)$ by the rational index $\bar{\Omega}_\theta(\gamma) = \sum_{d|\gamma} \frac{1}{d^2} \Omega_\theta(\frac{\gamma}{d})$ and insert a Boltzmann symmetry factor. *[Manschot BP Sen'11]*

Remarks

- In order to enforce Bose-Fermi statistics whenever two charges coincide, one should replace $\Omega_\theta(\gamma)$ by the rational index $\bar{\Omega}_\theta(\gamma) = \sum_{d|\gamma} \frac{1}{d^2}\Omega_\theta(\frac{\gamma}{d})$ and insert a Boltzmann symmetry factor. *[Manschot BP Sen'11]*
- When the charges γ_i are not linearly independent, some splittings can involve higher valency vertices. One can treat them using the full KS wall-crossing formula, or perturb θ such that only binary trees remain.

Remarks

- In order to enforce Bose-Fermi statistics whenever two charges coincide, one should replace $\Omega_\theta(\gamma)$ by the rational index $\bar{\Omega}_\theta(\gamma) = \sum_{d|\gamma} \frac{1}{d^2} \Omega_\theta(\frac{\gamma}{d})$ and insert a Boltzmann symmetry factor. *[Manschot BP Sen'11]*
- When the charges γ_i are not linearly independent, some splittings can involve higher valency vertices. One can treat them using the full KS wall-crossing formula, or perturb θ such that only binary trees remain.
- The attractor flow tree formula is consistent with wall-crossing: the index jumps when z crosses the wall $\mathcal{W}(\gamma_{L(v_0)}, \gamma_{R(v_0)})$ associated to the primary splitting for one of the trees.

Remarks

- There are additional ‘fake walls’ where the topology of the trees jump but the total index is constant, thanks to the identity

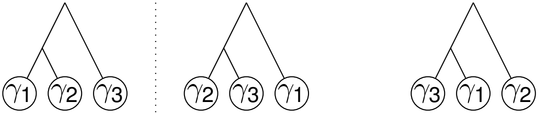

$$\langle\gamma_1,\gamma_2\rangle\,\langle\gamma_1+\gamma_2,\gamma_3\rangle+\mathrm{cyc.}=0$$

Remarks

- There are additional ‘fake walls’ where the topology of the trees jump but the total index is constant, thanks to the identity

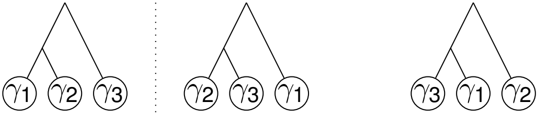

$$\langle \gamma_1, \gamma_2 \rangle \langle \gamma_1 + \gamma_2, \gamma_3 \rangle + \text{cyc.} = 0$$

- The formula can be refined by replacing

$$\begin{aligned} \langle \gamma_L, \gamma_R \rangle &\to \frac{y^{\langle \gamma_L, \gamma_R \rangle} - y^{-\langle \gamma_L, \gamma_R \rangle}}{y - 1/y} \\ \bar{\Omega}_\theta(\gamma) &\to \bar{\Omega}_\theta(\gamma, y) = \sum_{d|\gamma} \frac{y - 1/y}{d(y^d - y^{-d})} \Omega_\theta(\tfrac{\gamma}{d}, y^d) \end{aligned}$$

Physically, y is a fugacity conjugate to angular momentum in $\mathbb{R}^3$.

Flow tree formula from scattering diagrams

- For any quiver with potential (Q, W), the scattering diagram $\mathcal{D}$ is the set of real codimension-one rays $\{\mathcal{R}(\gamma), \gamma \in \mathbb{Z}^{Q_0}\}$ defined by *[Bridgeland'16]*

$$\mathcal{R}(\gamma) = \{\zeta \in \mathbb{R}^{Q_0} : (\zeta, \gamma) = 0, \Omega_\zeta(k\gamma) \neq 0 \text{ for some } k \geq 1\}$$

Flow tree formula from scattering diagrams

- For any quiver with potential (Q, W), the scattering diagram $\mathcal{D}$ is the set of real codimension-one rays $\{\mathcal{R}(\gamma), \gamma \in \mathbb{Z}^{Q_0}\}$ defined by *[Bridgeland'16]*

$$\mathcal{R}(\gamma) = \{\zeta \in \mathbb{R}^{Q_0} : (\zeta, \gamma) = 0, \Omega_\zeta(k\gamma) \neq 0 \text{ for some } k \geq 1\}$$

- Each point along $\mathcal{R}(\gamma)$ is endowed with an automorphism of the quantum torus algebra, (assume γ primitive)

$$\mathcal{U}(\gamma) = \exp\left(\sum_{m=1}^{\infty} \frac{\bar{\Omega}_\zeta(k\gamma, y)}{y^{-1} - y} \mathcal{X}_{k\gamma}\right) , \quad \mathcal{X}_\gamma \mathcal{X}_{\gamma'} = (-y)^{\langle \gamma, \gamma' \rangle} \mathcal{X}_{\gamma+\gamma'}$$

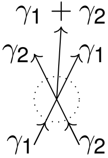

• The WCF ensures that the diagram is consistent, $\prod_{\gamma_i} \mathcal{U}(\gamma_i)^{\pm 1} = 1$ around any codimension 2 intersection. The Attractor Flow Tree Formula determines outgoing rays from incoming rays at each vertex. *[Argüz Bousseau '20]*.

Orbifold scattering diagram

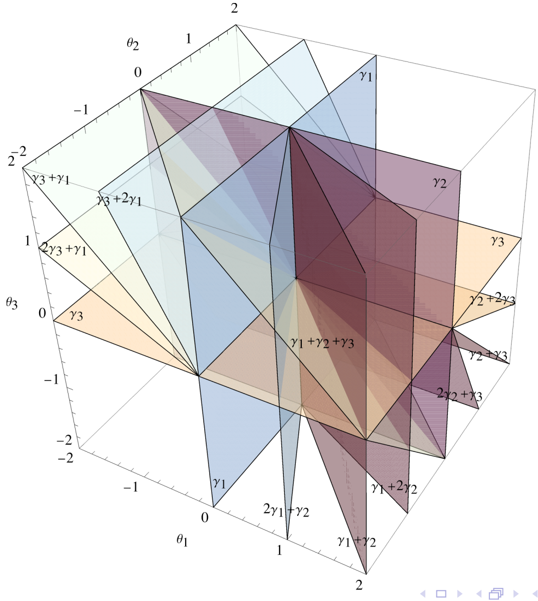

A 2D slice of the orbifold scattering diagram

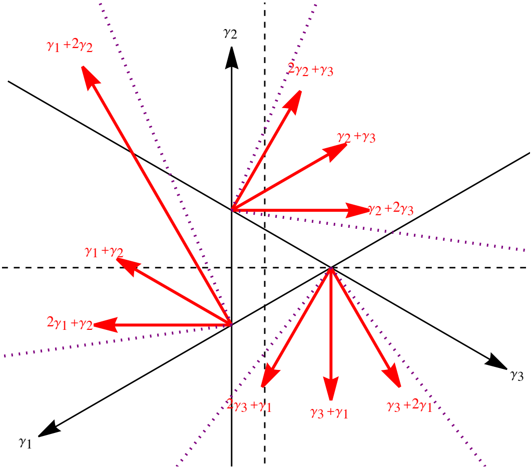

A 2D slice of the orbifold scattering diagram

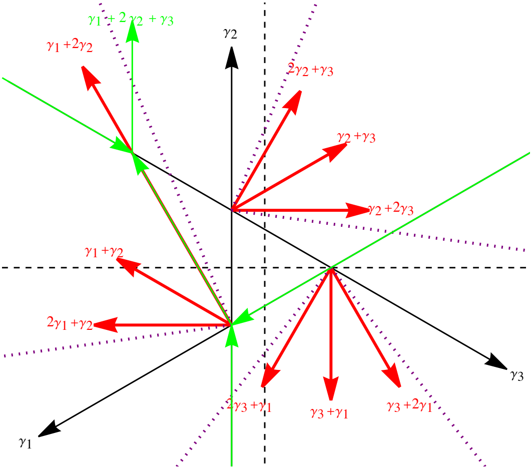

Flow trees from scattering diagrams

- More generally, for any $\psi \in \mathbb{R}/2\pi\mathbb{Z}$ define scattering rays as codimension-one loci in the space of Bridgeland stability conditions

$$\mathcal{R}_\psi(\gamma) = \{Z : \mathrm{Re}(e^{-\mathrm{i}\psi} Z(\gamma)) = 0, \mathrm{Im}(e^{-\mathrm{i}\psi} Z(\gamma)) > 0, \Omega_\zeta(k\gamma) \neq 0\}$$

Flow trees from scattering diagrams

- More generally, for any $\psi \in \mathbb{R}/2\pi\mathbb{Z}$ define scattering rays as codimension-one loci in the space of Bridgeland stability conditions

$$\mathcal{R}_\psi(\gamma) = \{Z : \mathrm{Re}(e^{-\mathrm{i}\psi} Z(\gamma)) = 0, \mathrm{Im}(e^{-\mathrm{i}\psi} Z(\gamma)) > 0, \Omega_\zeta(k\gamma) \neq 0\}$$

- For a non-compact CY3, $Z(\gamma)$ is holomorphic in Kähler moduli, thus arg $Z(\gamma)$ is constant along the gradient flow of $|Z(\gamma)|$. Choosing ψ such that $z \in \mathcal{R}_\psi(\gamma)$, edges of attractor flow trees lie inside $\mathcal{R}_\psi(\gamma_e)$, while vertices lie in $\mathcal{R}_\psi(\gamma_{L(v)}) \cap \mathcal{R}_\psi(\gamma_{R(v)})$.

Flow trees from scattering diagrams

- More generally, for any $\psi \in \mathbb{R}/2\pi\mathbb{Z}$ define scattering rays as codimension-one loci in the space of Bridgeland stability conditions

$$\mathcal{R}_\psi(\gamma) = \{Z : \mathrm{Re}(e^{-\mathrm{i}\psi} Z(\gamma)) = 0, \mathrm{Im}(e^{-\mathrm{i}\psi} Z(\gamma)) > 0, \Omega_\zeta(k\gamma) \neq 0\}$$

- For a non-compact CY3, $Z(\gamma)$ is holomorphic in Kähler moduli, thus arg $Z(\gamma)$ is constant along the gradient flow of $|Z(\gamma)|$. Choosing ψ such that $z \in \mathcal{R}_\psi(\gamma)$, edges of attractor flow trees lie inside $\mathcal{R}_\psi(\gamma_e)$, while vertices lie in $\mathcal{R}_\psi(\gamma_{L(v)}) \cap \mathcal{R}_\psi(\gamma_{R(v)})$.
- Besides, since $Z(\gamma)$ is holomorphic, initial rays must originate from attractor points on the boundary.

Flow trees from scattering diagrams

- More generally, for any $\psi \in \mathbb{R}/2\pi\mathbb{Z}$ define scattering rays as codimension-one loci in the space of Bridgeland stability conditions

$$\mathcal{R}_\psi(\gamma) = \{Z : \mathrm{Re}(e^{-\mathrm{i}\psi} Z(\gamma)) = 0, \mathrm{Im}(e^{-\mathrm{i}\psi} Z(\gamma)) > 0, \Omega_\zeta(k\gamma) \neq 0\}$$

- For a non-compact CY3, $Z(\gamma)$ is holomorphic in Kähler moduli, thus arg $Z(\gamma)$ is constant along the gradient flow of $|Z(\gamma)|$. Choosing ψ such that $z \in \mathcal{R}_\psi(\gamma)$, edges of attractor flow trees lie inside $\mathcal{R}_\psi(\gamma_e)$, while vertices lie in $\mathcal{R}_\psi(\gamma_{L(v)}) \cap \mathcal{R}_\psi(\gamma_{R(v)})$.
- Besides, since $Z(\gamma)$ is holomorphic, initial rays must originate from attractor points on the boundary.
- Fflow trees are subsets of scattering diagrams, determining sequences of scatterings which produce an outgoing ray $\mathcal{R}_\psi(\gamma)$ passing through the desired point z.

Outline

Large volume scattering diagram

- For the large volume stability conditions $Z^{LV}_{(s,t)}$, *[Bousseau'19]* constructed the scattering diagram $\mathcal{D}_\psi$ in (s,t) upper half-plane for $\psi = 0$. For $\psi \neq 0$, just map $(s,t) \mapsto (s - t\tan\psi, t/\cos\psi)$.

Large volume scattering diagram

- For the large volume stability conditions $Z^{LV}_{(s,t)}$, [Bousseau'19] constructed the scattering diagram $\mathcal{D}_\psi$ in (s,t) upper half-plane for $\psi = 0$. For $\psi \neq 0$, just map $(s,t) \mapsto (s - t\tan\psi, t/\cos\psi)$.
- The rays $\mathcal{R}(\gamma)$ are branches of hyperbola asymptoting to $t = \pm(s - \frac{d}{r})$ for $r \neq 0$, or vertical lines when $r = 0$. Walls of marginal stability $\mathcal{W}(\gamma, \gamma')$ are half-circles centered on real axis.

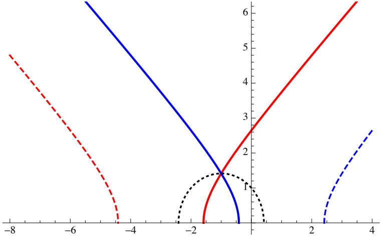

Large volume scattering diagram

- For the large volume stability conditions $Z^{LV}_{(s,t)}$, [Bousseau'19] constructed the scattering diagram $\mathcal{D}_\psi$ in (s,t) upper half-plane for $\psi = 0$. For $\psi \neq 0$, just map $(s,t) \mapsto (s - t\tan\psi, t/\cos\psi)$.
- The rays $\mathcal{R}(\gamma)$ are branches of hyperbola asymptoting to $t = \pm(s - \frac{d}{r})$ for $r \neq 0$, or vertical lines when $r = 0$. Walls of marginal stability $\mathcal{W}(\gamma,\gamma')$ are half-circles centered on real axis.

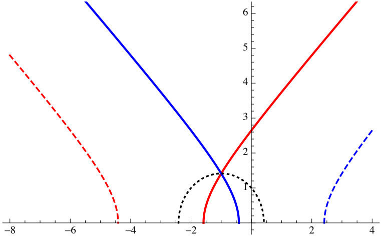

- Think of $\mathcal{R}(\gamma)$ as the worldline of a fictitious particle of charge r, mass $m^2 = \frac{1}{2}d^2 - r\,\mathrm{ch}_2$ moving in a constant electric field !

Large volume scattering diagram

- Initial rays correspond to $\mathcal{O}(m)$ and $\mathcal{O}(m)[1]$, *ie* (anti)D4-branes with m units of flux, emanating from $(s,t) = (m,0)$ on the boundary where the central charge vanishes.

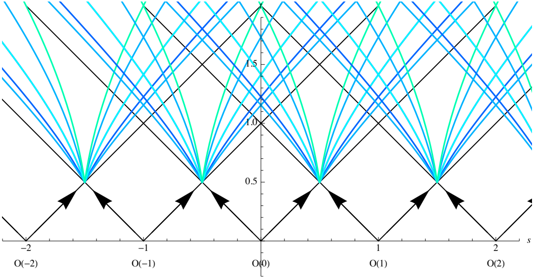

Large volume scattering diagram

- Initial rays correspond to $\mathcal{O}(m)$ and $\mathcal{O}(m)[1]$, *ie* (anti)D4-branes with m units of flux, emanating from $(s,t)=(m,0)$ on the boundary where the central charge vanishes.

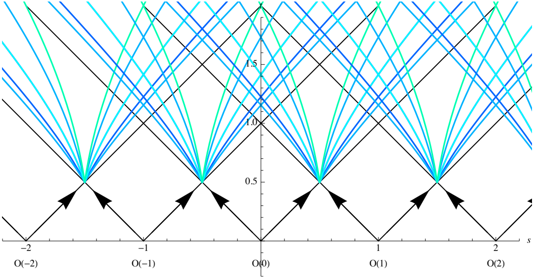

- The first scatterings occur for $t \geq \frac{1}{2}$, after each constituent has moved by $|\Delta s| \geq \frac{1}{2}$. Causality and monotonicity of the 'electric potential' $\varphi(\gamma) = d - sr$ along the flow, allow to bound the number and charges of constituents.

Flow trees for $\gamma = [0, 4, 1]$

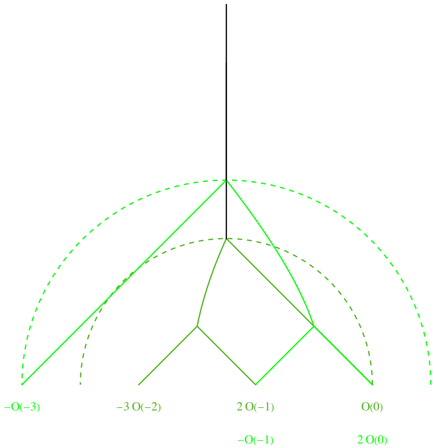

- $\{\{-3\mathcal{O}(-2), 2\mathcal{O}(-1)\}, \mathcal{O}\}$:
  $3\mathcal{O}(-2) \to 2\mathcal{O}(-1) \oplus \mathcal{O} \to E$
  $K_3(2,3)K_{12}(1,1) \to -156$
- $\{-\mathcal{O}(-3), \{-\mathcal{O}(-1), 2\mathcal{O}\}\}$:
  $\mathcal{O}(-3) \oplus \mathcal{O}(-1) \to 2\mathcal{O} \to E$
  $K_3(1,2)K_{12}(1,1) \to -36$

Total: $\Omega_\infty(\gamma) = -192 = GV_4^{(0)}$

Flow trees for $\gamma = [1, 0, -3)$

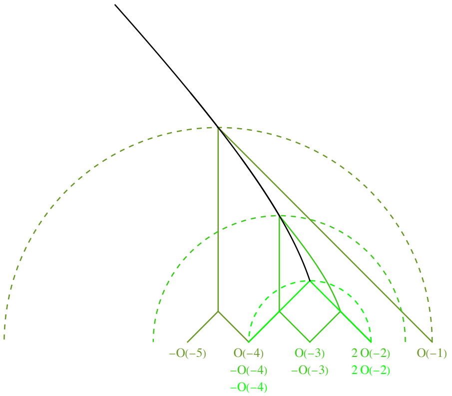

- $\{\{-\mathcal{O}(-5), \mathcal{O}(-4)\}, \mathcal{O}(-1)\}$
  $\mathcal{O}(-5) \to \mathcal{O}(-4) \oplus \mathcal{O}(-1) \to E$
  $K_3(1,1)^2 \to 9$
- $\{\{-\mathcal{O}(-4), \mathcal{O}(-3)\},$
  $\{-\mathcal{O}(-3), 2\mathcal{O}(-2)\}\}$
  $\mathcal{O}(-4) \oplus \mathcal{O}(-3) \to$
  $\mathcal{O}(-3) \oplus 2\mathcal{O}(-2) \to E$
  $K_3(1,1)^2 K_3(1,2) \to 27$
- $\{-\mathcal{O}(-4), 2\mathcal{O}(-2)\}$
  $\mathcal{O}(-4) \to 2\mathcal{O}(-2) \to E$
  $K_6(1,2) \to 15$

Total: $\Omega_\infty(\gamma) = 51 = \chi(\mathrm{Hilb}_4 \mathbb{P}^2)$

Outline

Exact scattering diagram

- The full scattering diagram should interpolate between $\mathcal{D}_\psi^{\rm LV}$ around $\tau = \mathrm{i}\infty$ and $\mathcal{D}_\psi^{o}$ around $\tau = \tau_o$, and be invariant under the action of $\Gamma_1(3)$.

Exact scattering diagram

- The full scattering diagram should interpolate between $\mathcal{D}_\psi^{\mathrm{LV}}$ around $\tau = \mathrm{i}\infty$ and $\mathcal{D}_\psi^{o}$ around $\tau = \tau_o$, and be invariant under the action of $\Gamma_1(3)$.
- Under $\tau \mapsto \frac{\tau}{3n\tau+1}$ with $n \in \mathbb{Z}$, $\mathcal{O} \mapsto \mathcal{O}[n]$. Hence we have an doubly infinite family of initial rays associated to $\mathcal{O}(m)[n]$.

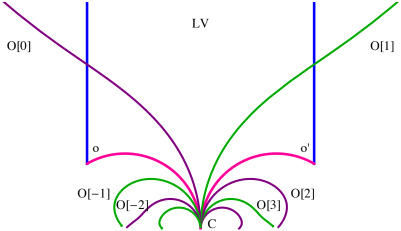

Exact scattering diagram

- The full scattering diagram should interpolate between $\mathcal{D}_\psi^{\rm LV}$ around $\tau = {\rm i}\infty$ and $\mathcal{D}_\psi^{o}$ around $\tau = \tau_o$, and be invariant under the action of $\Gamma_1(3)$.
- Under $\tau \mapsto \frac{\tau}{3n\tau+1}$ with $n \in \mathbb{Z}$, $\mathcal{O} \mapsto \mathcal{O}[n]$. Hence we have an doubly infinite family of initial rays associated to $\mathcal{O}(m)[n]$.

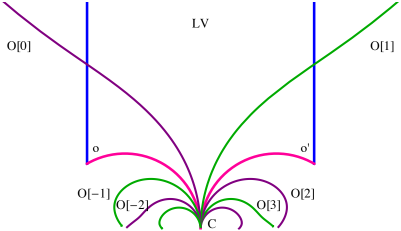

- For $|\tan\psi| < \frac{1}{2\mathcal{V}}$ where $\mathcal{V} = {\rm Im}\, T(0) = \frac{27}{4\pi^2} {\rm Im Li}_2(e^{2\pi {\rm i}/3}) \simeq 0.463$ only the rays associated to $\mathcal{O}(m)[0]$ and $\mathcal{O}(m)[1]$ escape to ${\rm i}\infty$, and merge onto rays in the large volume scattering diagram $\mathcal{D}_\psi^{\rm LV}$.

Exact scattering diagram - $\psi = 0$

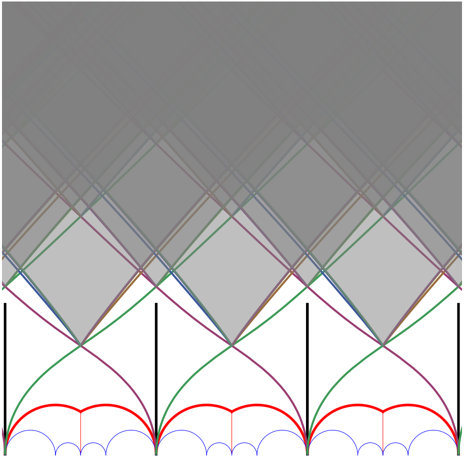

Exact scattering diagram

- In addition, there must be an infinite family of initial rays coming from $\tau = \frac{p}{q}$ with $q \neq 0 \mod 3$, corresponding to $\Gamma_1(3)$-images of $\mathcal{O}(0)$.

Exact scattering diagram

- In addition, there must be an infinite family of initial rays coming from $\tau = \frac{p}{q}$ with $q \neq 0 \mod 3$, corresponding to $\Gamma_1(3)$-images of $\mathcal{O}(0)$.
- This includes initial rays emitted at $\tau = n - \frac{1}{2}$, associated to $\Omega(n+1)$; for $\psi \sim \frac{\pi}{2}$, these merge onto initial rays of the orbifold scattering diagram.

Exact scattering diagram

- In addition, there must be an infinite family of initial rays coming from $\tau = \frac{p}{q}$ with $q \neq 0 \mod 3$, corresponding to $\Gamma_1(3)$-images of $\mathcal{O}(0)$.
- This includes initial rays emitted at $\tau = n - \frac{1}{2}$, associated to $\Omega(n+1)$; for $\psi \sim \frac{\pi}{2}$, these merge onto initial rays of the orbifold scattering diagram.
- We conjecture that the only initial rays are the $\Gamma_1(3)$ images of the structure sheaf $\mathcal{O}$, each of them carrying $\Omega(k\gamma) = 1$ for $k = 1$, 0 otherwise.

Exact scattering diagram - $\psi = \pm\frac{\pi}{2} \mod 2\pi$

- For $\psi = \pm\frac{\pi}{2}$, the diagram $\mathcal{D}^{\Pi}_{\psi}$ simplifies dramatically, since the loci $\mathrm{Im} Z_\tau(\gamma) = 0$ are lines of constant $s := \frac{\mathrm{Im}\, T_D}{\mathrm{Im}\, T} = \frac{d}{r}$.

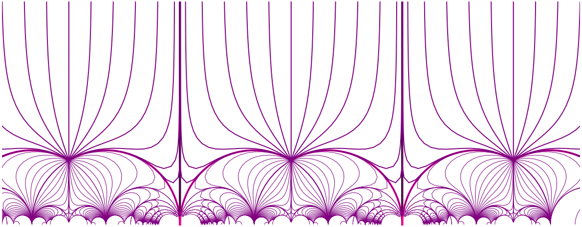

Exact scattering diagram - $\psi = \pm\frac{\pi}{2} \mod 2\pi$

- For $\psi = \pm\frac{\pi}{2}$, the diagram $\mathcal{D}^{\Pi}_{\psi}$ simplifies dramatically, since the loci $\mathrm{Im} Z_\tau(\gamma) = 0$ are lines of constant $s := \frac{\mathrm{Im}\, T_D}{\mathrm{Im}\, T} = \frac{d}{r}$.

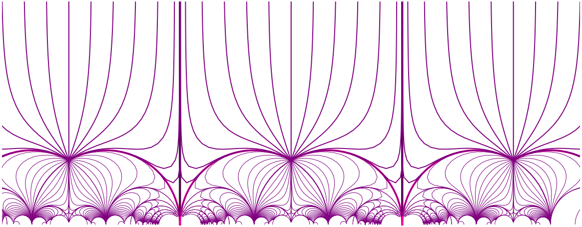

- Hence, there is no wall-crossing between τ_o and $\tau = \mathrm{i}\infty$ when $-1 \leq \frac{d}{r} \leq 0$, explaining why the Gieseker index $\Omega_\infty(\gamma)$ agrees with the index $\Omega_c(\gamma)$ in the anti-attractor chamber.

Exact scattering diagram, varying ψ

$\gamma = [0, 1, 1) = \text{ch}\, \mathcal{O}_C$:

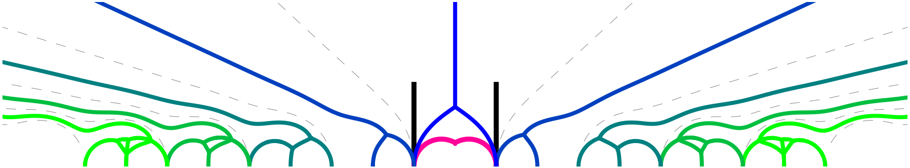

$\gamma = [1, 0, 1) = \text{ch}\, \mathcal{O}$:

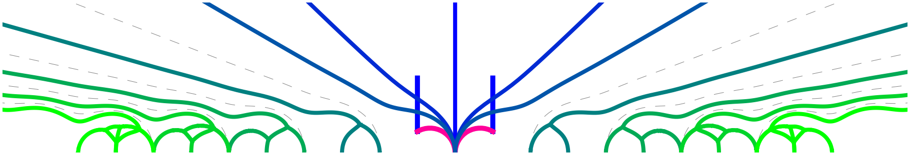

Conclusion - outlook

- The scattering diagram is the proper mathematical framework for the attractor flow tree formula in the case of local CY3. This is because $Z(\gamma)$ is holomorphic on $\mathcal{M}_K$, so the gradient flow preserves the phase of $Z(\gamma)$. Moreover, initial rays can only start from the boundary.

Conclusion - outlook

- The scattering diagram is the proper mathematical framework for the attractor flow tree formula in the case of local CY3. This is because $Z(\gamma)$ is holomorphic on $\mathcal{M}_K$, so the gradient flow preserves the phase of $Z(\gamma)$. Moreover, initial rays can only start from the boundary.
- This provides an effective way of computing (unframed) BPS invariants in any chamber, and a natural decomposition into elementary constituents. Mathematically, different trees should correspond to different strata in $\mathcal{M}_Z(\gamma)$.

Conclusion - outlook

- The scattering diagram is the proper mathematical framework for the attractor flow tree formula in the case of local CY3. This is because $Z(\gamma)$ is holomorphic on $\mathcal{M}_K$, so the gradient flow preserves the phase of $Z(\gamma)$. Moreover, initial rays can only start from the boundary.
- This provides an effective way of computing (unframed) BPS invariants in any chamber, and a natural decomposition into elementary constituents. Mathematically, different trees should correspond to different strata in $\mathcal{M}_Z(\gamma)$.
- It would be interesting to extend this description to other toric CY3, such as local del Pezzo surfaces, and to framed BPS indices.

Conclusion - outlook

- The scattering diagram is the proper mathematical framework for the attractor flow tree formula in the case of local CY3. This is because $Z(\gamma)$ is holomorphic on $\mathcal{M}_K$, so the gradient flow preserves the phase of $Z(\gamma)$. Moreover, initial rays can only start from the boundary.
- This provides an effective way of computing (unframed) BPS invariants in any chamber, and a natural decomposition into elementary constituents. Mathematically, different trees should correspond to different strata in $\mathcal{M}_Z(\gamma)$.
- It would be interesting to extend this description to other toric CY3, such as local del Pezzo surfaces, and to framed BPS indices.
- For a compact CY3, $\arg Z(\gamma)$ is no longer constant along the flow and there can be attractor points with $\Omega_\star(\gamma) \neq 0$ at finite distance in Kähler moduli space...

Thanks for your attention !